ORIGINAL ARTICLE

Plant, Cell & Environment | PCE | WILEY

SlNAC3 suppresses cold tolerance in tomatoes by enhancing ethylene biosynthesis

Tao Wang[1] | **Xuemin Ma[2]** (ID) | **Ying Chen[1]** | **Cuicui Wang[1]** | **Zhenxiao Xia[1]** | **Zixi Liu[1]** | **Lihong Gao[1]** | **Wenna Zhang[1]** (ID)

[1]Beijing Key Laboratory of Growth and Developmental Regulation for Protected Vegetable Crops, China Agricultural University, Beijing, China

[2]Umeå Plant Science Centre, UMEÅ, Sweden

Correspondence
Wenna Zhang, Beijing Key Laboratory of Growth and Developmental Regulation for Protected Vegetable Crops, China Agricultural University, 100193, Beijing, China.
Email: zhangwenna@cau.edu.cn

Abstract

Low temperature stress poses a significant challenge to the productivity of horticultural crops. The dynamic expression of cold-responsive genes plays a crucial role in plant cold tolerance. While NAC transcription factors have been extensively studied in plant growth and development, their involvement in regulating plant cold tolerance remains poorly understood. In this study, we focused on the identification and characterisation of *SlNAC3* as the most rapid and robust responsive gene in tomato under low temperature conditions. Manipulating *SlNAC3* through overexpression or silencing resulted in reduced or enhanced cold tolerance, respectively. Surprisingly, we discovered a negative correlation between the expression of *CBF* and cold tolerance in the *SlNAC3* transgenic lines. These findings suggest that SlNAC3 regulates tomato cold tolerance likely through a CBF-independent pathway. Furthermore, we conducted additional investigations to identify the molecular mechanisms underlying SlNAC3-mediated cold tolerance in tomatoes. Our results revealed that SlNAC3 controls the transcription of ethylene biosynthetic genes, thereby bursting ethylene release in response to cold stress. Indeed, the silencing of these genes led to an augmentation in cold tolerance. This discovery provides valuable insights into the regulatory pathways involved in ethylene-mediated cold tolerance in tomatoes, offering potential strategies for developing innovative approaches to enhance cold stress resilience in this economically important crop species.

KEYWORDS
cold response, NAC transcription factor

1 | INTRODUCTION

Low temperature stress is a prevalent environmental challenge that can negatively impact plant cell membrane permeability and photosynthetic activity, thereby inhibiting overall plant growth and development. In response to low temperature stress, plants activate a range of cold-responsive genes (Ding et al., 2019; Larran et al., 2023). One of the extensively researched transcription factors in the field of plant cold responses is the C-repeat binding factor/dehydration-responsive element binding protein 1 (CBF/DREB1). CBF/DREB1 has a specific affinity for the CRT/DRE sequence found

in the promoter region of cold-responsive genes (COR). This binding interaction triggers the transcriptional activation of COR genes (Baker et al., 2022; Liu et al., 1998; Stockinger et al., 1997). Besides the CBF-dependent pathway, there are also genes independent of the CBF pathway that play significant roles in enhancing plant cold tolerance (Li et al., 2017; Zhao et al., 2016).

Tomato is a warm-temperature vegetable that is sensitive to low temperatures. Low temperature negatively affects tomato flowering, fruit development, and ripening. In our previous studies, we found that the tomato SlNAC3 transcription factor responds to various abiotic stresses, including drought, and salt stress (Han et al., 2012).

The NAC (NAM, ATAF1/2, and CUC2) transcription factor family is exclusive to plants. In tomato (*Solanum lycopersicum*), there have been 101 identified member genes of the NAC family. The N-terminal region of NAC proteins is highly conserved and exhibits specific binding to the promoters of target genes, while the variable C-terminal region determines their transcriptional activation or repression activity (Puranik et al., 2012).

NAC transcription factors play diverse regulatory roles in plant growth and development, encompassing seed germination, lateral root and secondary cell wall formation, organ development, and senescence (Christiansen and Gregersen, 2014; Olsen et al., 2005; Ricachenevsky et al., 2013; Wang et al., 2022; Zhong et al., 2010). Furthermore, accumulating evidence suggests that NAC family genes also participate in the response to both biotic and abiotic stresses in plants. They can be induced by various environmental factors, including low temperature, drought, bacterial invasion, and mechanical damage. For example, GmNAC20 regulates cold tolerance in soybean (*Glycine max*) by participating in the CBF-COR pathway (Hao et al., 2011). MaNAC1 enhances cold resistance in banana (*Musa acuminata*) through CBF (Shan et al., 2014). MdNAC047, through interaction with the ethylene response factor MdERF3, modulates salt stress tolerance in apple (*Malus sieversii*) (An et al., 2018). SlNAC2 positively regulates tomato cold tolerance by reducing ROS accumulation and inducing CBF1 transcription (Ma et al., 2013). In *Oryza sativa*, overexpression of ONAC022 or OsNAC045 leads to abiotic stress tolerance (Hong et al., 2016; Zhang et al., 2020). However, limited information is available on the mechanism by which NAC transcription factors mediate cold resistance in tomato.

Ethylene is a gaseous plant hormone that is increasingly recognised for its roles in plant cold tolerance (Huang et al., 2023). In the synthesis pathway of ethylene, two key enzymes, 1-aminocyclopropane-1-carboxylate synthase (ACS) and 1-aminocyclopropane-1-carboxylic acid oxidase (ACO), play crucial regulatory roles in ethylene production (Pattyn et al., 2021). Furthermore, ethylene has been reported to be involved in stress responses mediated by NAC transcription factors in plants. For instance, AtNAC2 increases its expression level to participate in the ethylene-regulated salt stress response (He et al., 2005). The CaNAC1 transcription factor in pepper exhibits elevated expression levels under exogenous ethylene induction (Oh et al., 2005), and ethylene treatment induces the expression of the wheat TaNAC4 gene (Xia et al., 2010). Gaining a better understanding of the intricate interplay between ethylene signalling, the NAC transcription factor, and cold tolerance in tomato plants holds significant promise for uncovering the underlying molecular mechanisms.

In this study, our initial focus was to assess the expression levels of various NAC genes under low temperature stress. Among them, *SlNAC3* exhibited the most rapid and robust response to low temperature. Manipulating *SlNAC3* through overexpression or silencing resulted in reduced or enhanced cold tolerance, respectively. However, we observed a negative correlation between *CBF* expression and cold tolerance in the transgenic lines overexpressing *SlNAC3*. This led us to speculate that SlNAC3 regulates tomato cold tolerance through a CBF-independent pathway. Subsequently, we identified and validated that SlNAC3 controls the transcription of ethylene biosynthetic genes, thereby positively regulating ethylene release and negatively modulating cold tolerance in tomato plants. This study provides further understanding of the regulatory pathways involved in ethylene-mediated cold tolerance in tomatoes, contributing to the development of innovative strategies for enhancing cold stress resilience in this important crop species.

2 | RESULTS

2.1 | Tomato NAC transcription factor family member SlNAC3 responds to cold stress

There have been few reports on the function of NAC transcription factors in cold stress. We aimed at identifying a key NAC transcription factor involved in the early cold response. In the transcriptome database generated in our lab, we found 14 genes in the tomato NAC transcription factor family with significant expression variations after 2 h of 4°C cold stress. Their expression levels was further analyzed upon 4°C cold stress for 2, 6, 12 and 24 h. Among them, the expression level of *SlNAC3* showed the most outstanding change after 2 h cold stress (Figure 1a). Therefore, we focused primarily on the role of SlNAC3 in low-temperature stress. We then examined the expression levels of *SlNAC3* at more time points during 4°C low-temperature treatment. We found that the expression level of the *SlNAC3* gene was significantly higher at 2 h compared to 0 h, and it subsequently decreased after 2 h. Within 1 day of 4°C low-temperature treatment, the expression level at 2 h was the highest among the time points examined (Figure 1b). These results indicate that *SlNAC3* is involved in an early response to 4°C low-temperature stress.

Previous studies have demonstrated the important roles of many NAC genes in tomato growth and development processes. SlNAC3 participates in tomato fruit ripening and carotenoid biosynthesis. We analyzed the expression pattern of SlNAC3 in different tomato tissues and found that it exhibits the highest expression levels in flowers and fruits, while showing relatively lower expression levels in the vegetative organs, including roots, stems, and leaves (Figure 1c). It remains obscure whether SlNAC3 is involved in cold tolerance at the phase of vegetative growth.

2.2 | SlNAC3 negatively regulates cold tolerance in tomato

To study the role of SlNAC3 in plant cold tolerance, we generated *SlNAC3* overexpression lines and knockout lines in the Micro Tom background. We obtained three overexpression lines, namely *SlNAC3*-OE#4, OE#5, and OE#7 (Figure S1a), and also two CRISPR/Cas9 knockout lines, namely slnac3#2, slnac3#13 (Figure S1d). We detected the accumulation of *SlNAC3* transcripts and protein in these three overexpression transgenic plants using
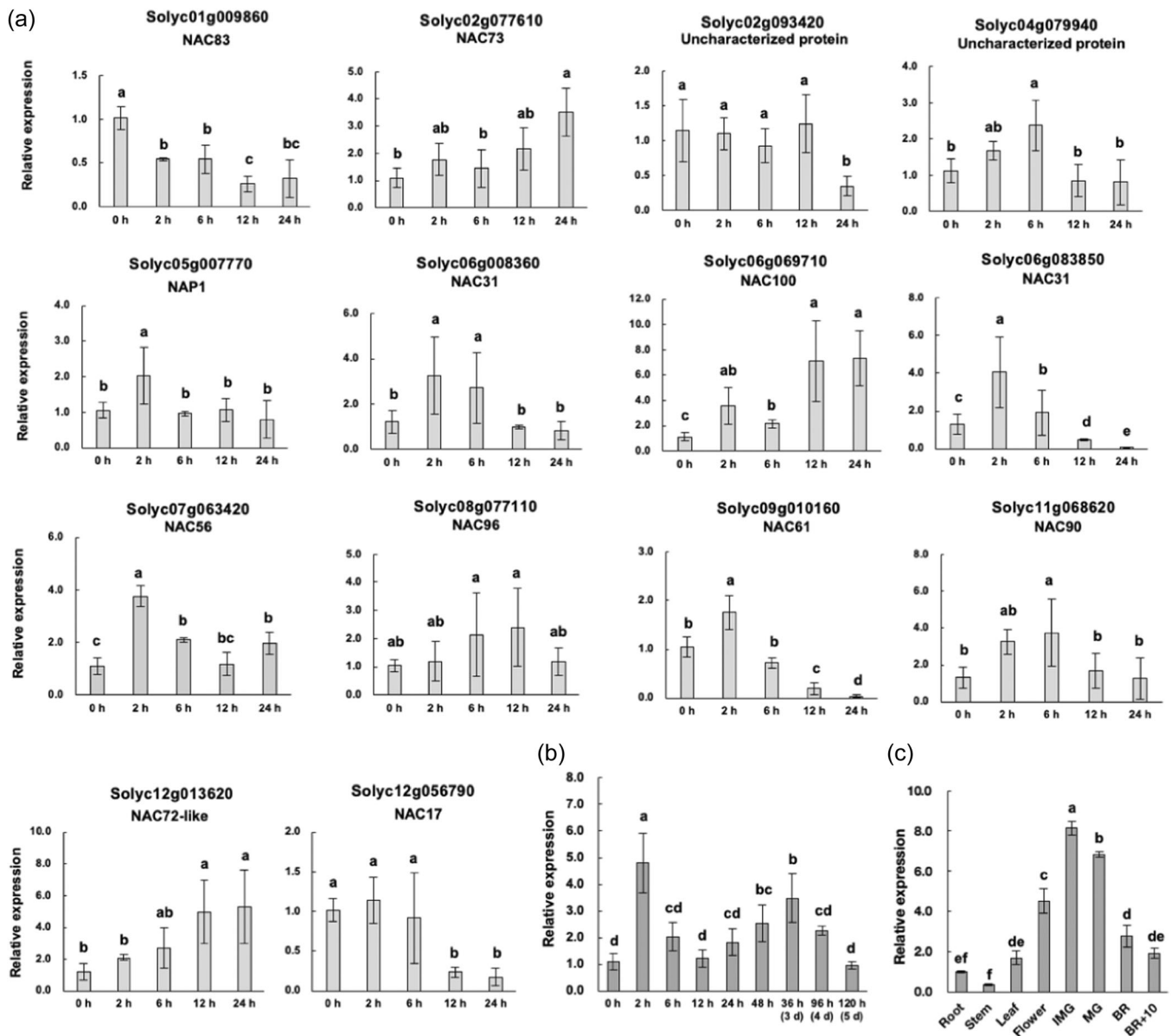
FIGURE 1 *SlNACs* in response to cold stress. (a) Relative expression levels of 14 *NAC* genes in tomato tested by RT-qPCR using *EF-1α* as the reference gene under cold stress (4°C) for 2, 6, 12, and 24 h. The data are shown as the means of three independent biological replicates, with each replicate consisting of 5–6 individual plants. Error bars represent standard deviations of three independent biological replicates. Lowercase letters on the graphs indicate significant differences ($p < 0.05$, Duncan's test). (b) Relative expression levels of *SlNAC3* gene were tested by RT-qPCR using *EF-1α* as the reference gene under cold stress (4°C) for 5 days. The data are shown as the means of three independent biological replicates, with each replicate consisting of 5–6 individual plants. Error bars represent standard deviations of three independent biological replicates. Lowercase letters on the graphs indicate significant differences ($p < 0.05$, Duncan's test). (c) Relative expression levels of *SlNAC3* gene in different tissues of tomato plants were tested by RT-qPCR using *EF-1α* as the reference gene. IMG, immature green; MG, mature green; Br, breaker; B + 10, 10 days after breaker. The data are shown as the means of three independent biological replicates, with each replicate consisting of 5–6 individual plants. Error bars represent standard deviations of three independent biological replicates. Lowercase letters on the graphs indicate significant differences ($p < 0.05$, Duncan's test).

RT-qPCR and Western blot analysis, respectively. The results showed a significant increase in the expression levels of *SlNAC3* in all three overexpression lines, and the expression of the SlNAC3::GFP fusion protein was detected (Figure S1b,c). Additionally, we verified the genomic sequence of the first exon of *SlNAC3*, comparing with wild type, the knockout lines showed overlapped

peaks in the CRISPR/Cas9 targeting region, proving both of them were *SlNAC3* knockout mutants (Figure S1d).

When tomato plants reached the six-leaf stage, they were subjected to 4°C cold stress for 5 days. On the third day of cold treatment, the wild-type plants exhibited noticeable leaf curling and wilting at the leaf margins. The *SlNAC3* overexpression lines showed

more severe leaf curling and yellowing than the wild type. By the fifth day, the overexpression lines displayed overall dwarfing and wilting, while the wild-type plants exhibited pronounced leaf curling and yellowing at the leaf margins. Surprisingly, there wasn't any noticeable variation in cold injury between the two knockout lines and the wild type Micro Tom plants. The phenotypic analysis indicated that overexpression of *SlNAC3* reduced the resistance of tomato plants to 4°C cold stress (Figure 2a).

Additionally, physiological measurements related to cold stress were conducted on the plants at four time points during the 4°C cold stress. The results showed that the relative conductivity, MDA (malondialdehyde) content, and peroxide levels of the three over-expression lines were significantly higher than those of the wild-type plants on the third and fifth days of cold treatment. The Fv/Fm values of the overexpression lines were significantly lower than those of the wild-type plants. In contrast, there was no significant difference in relative conductivity, MDA content, peroxide levels and Fv/Fm values between the knockout lines and the wild-type plants (Figure 2b–g), consistent with the observed phenotypes. After 5 days of 4°C cold treatment, the plants were allowed to recover for 5 days at 25°C, and the phenotypes were observed. It was found that all plants showed some degree of recovery from cold damage, and the wild-type plants exhibited greater plant height and leaf area compared to the overexpression plants (Figure 2h,i).

Micro-Tom carries mutations in the SP and D genes, leading to a reduced response to GA and BR. This dwarf phenotype makes it less susceptible to exhibiting symptoms of dehydration and chilling injury (Marti et al., 2006). Therefore, we also conducted the same 4°C cold stress experiment using *SlNAC3* knockout homozygous lines, CR-NOR-like1#1 and CR-NOR-like1#11, which were generated previously in the background of Ailsa Craig. On the third day of the cold treatment, the leaves of wild-type plants exhibited noticeable curling and wilting compared to the knockout plants. By the fifth day, the cold damage symptoms were more pronounced in wild-type plants, with some even showing stem bending and lodging. Phenotypic analysis of the plants revealed that the knockout lines exhibited greater cold tolerance compared to the wild-type plants, indicating that the knockout of *SlNAC3* enhances tomato's resistance to 4°C cold temperature (Figure 3a). The determination of cold-related physiological indicators also supported the same conclusion (Figure 3b–g). After 5 days of 4°C cold treatment, the plants were subsequently allowed to recover in a 25°C environment for 5 days. The observations showed a certain degree of recovery in cold-induced symptoms in all plants, and the knockout plants exhibited significantly taller stature and larger leaf area compared to the wild-type plants (Figure 3h,i).

2.3 | Expression of cold-responsive genes regulated by SlNAC3

To investigate the mechanism underlying the SlNAC3 function in tomato plant cold tolerance, we analyzed the expression levels of

different cold-responsive genes in *SlNAC3* overexpression, and wild-type tomato plants backgrounded in Micro Tom using RT-qPCR. The results showed that the majority of genes had higher transcription levels in the overexpression plants compared to the wild-type plants (Figure 4a–c and Figure S2A). It has been widely documented that the expression levels of these genes are positively correlated with cold tolerance. However, our observation of decreased cold tolerance in *SlNAC3* overexpression plants contradicts these findings. Particularly, the CBF genes in the CBF pathway, which have been proven to be positively correlated with plant cold tolerance, showed the highest expression levels in *SlNAC3* overexpression plants. We also analyzed the expression levels of relevant genes in knockout and wild-type tomato plants backgrounded in both Micro Tom and Ailsa Craig. The results revealed that *CBF1-4*, and their associated *COR* genes had lower transcription levels in the cold-tolerant knockout plants compared to the wild-type plants (Figure 4b,c and Figure S3). Therefore, we speculated the role of SlNAC3 in other pathways associated with cold responses, and began exploring other potential cold resistance pathways in which SlNAC3 may be involved.

2.4 | SlNAC3 binds to the promoters of *SlACO1*, *SlACS2* and *SlACS4*, regulating ethylene biosynthesis

Numerous studies have reported that NAC transcription factor family genes can influence tomato fruit ripening and softening by participating in the ethylene synthesis pathway (Gao et al., 2018). Additionally, in some species, increased ethylene content has been shown to reduce plant cold tolerance, suggesting that *SlNAC3* may affect plant cold tolerance by modulating genes in the ethylene synthesis pathway (Huang et al., 2023). Therefore, we investigated the expression levels of various genes involved in the ethylene biosynthesis pathway across three overexpression (OE) lines. Notably, within the *SlNAC3*-OE lines, a significant upregulation was observed in several ACOs and ACSs, specifically ACO1/3/4/5 and ACS1A/1B/2/3/4/7 (Figure 5a and S4a). Within the *SlNAC3* knockout lines, a significant downregulation was observed in several ACOs and ACSs, specifically ACO1/2/3/4/6 and ACS1A/1B/2/4/6 (Figure 5b and S4b). Furthermore, we performed an in-depth analysis of the temporal gene expression patterns during a cold stress time course. Remarkably, a substantial portion of these genes exhibited a similar expression profile to that of *SlNAC3* (Figure 5c). They were promptly induced 2–12 h following cold treatment and subsequently repressed after 24 h, with the exception of ACS2 (Figure S4C). It is worth noting that ACS2/4 have been established as transcriptional targets of SlNAC3 during the process of fruit ripening (Gao et al., 2018). As a result, our focus was primarily directed towards the ACO genes, with the intention of identifying additional potential targets regulated by SlNAC3.

Analysis of the promoter sequences revealed the presence of NAC transcription factor binding motifs ("CACG") within the up-stream region of 1.5 kb (Figure 5d). Based on these findings, we selected *SlACO1*, *SlACO3*, *SlACO4* downstream candidate genes for
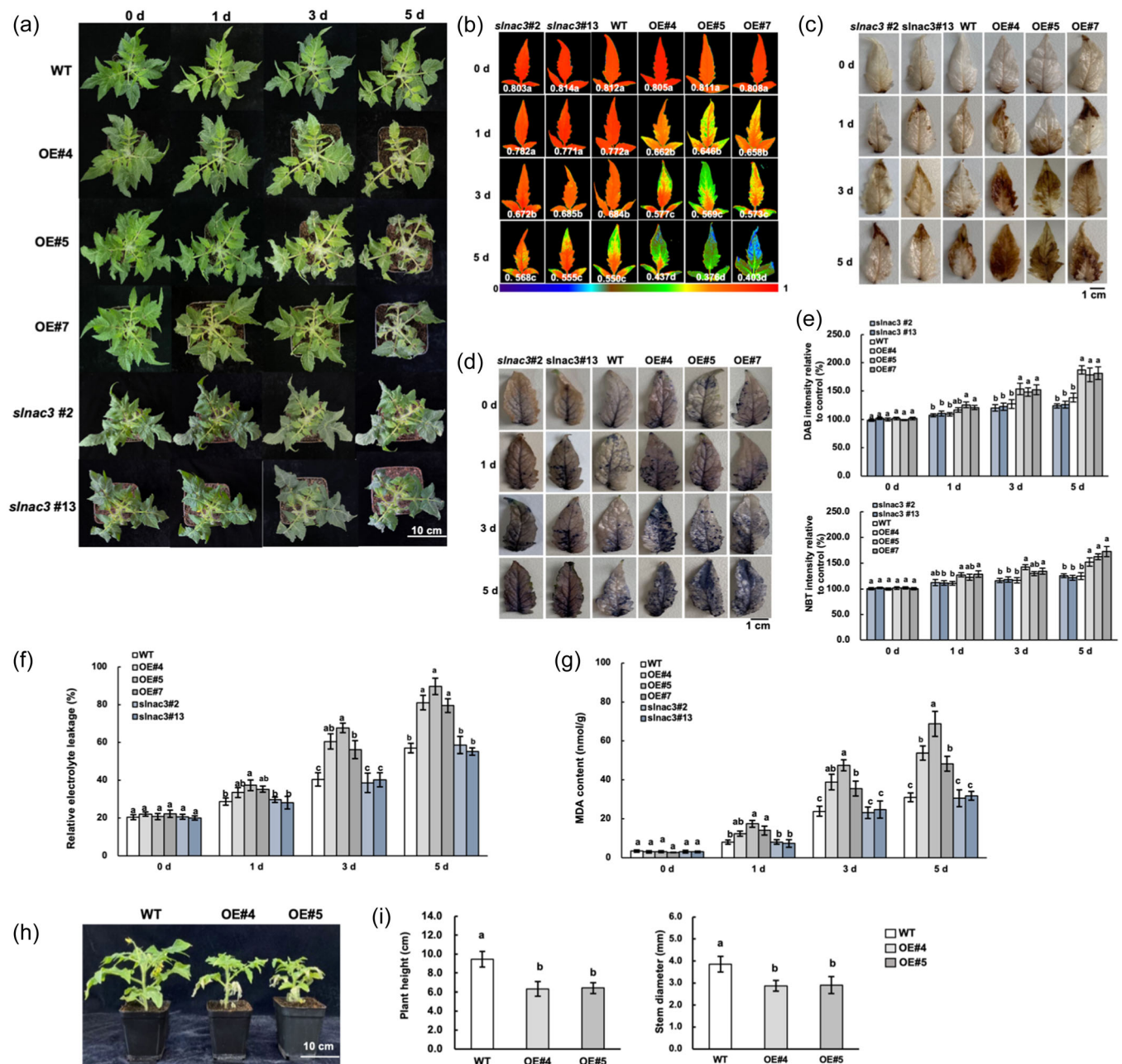
FIGURE 2 Phenotypic and physiological changes of Micro-Tom WT and *SlNAC3*-overexpressing tomato under different times of cold stress. (a) Phenotypes of Micro-Tom WT, *SlNAC3*-overexpressing lines (OE#4/5/7) and *SlNAC3* CRISPR/Cas9 knock-out lines (*slnac3* #2/13) under different times of cold stress (4°C). Scale bar = 5 cm. (b) Fv/Fm (maximum quantum yield of PSII) of Micro-Tom WT, *SlNAC3*-overexpressing lines (OE#4/5/7) and *SlNAC3* CRISPR/Cas9 knock-out lines (*slnac3* #2/13) under different times of cold stress (4°C). The colour change bar depicted at the bottom of image represents the degree of damage in the leaves. Lowercase letters indicate more severe damage in the leaves. (c) DAB (3,3'-diaminobenzidine), (d) Nitro blue tetrazolium (NBT) staining of tomato leaves and (e) Intensity of DAB and NBT staining relative to control (*slnac3* #2 at 0 day) of Micro-Tom WT, *SlNAC3*-overexpressing lines (OE#4/5/7) and *SlNAC3* CRISPR/Cas9 knock-out lines (*slnac3* #2/13) under different times of cold stress (4°C). The blue colour on the leaves represents the degree of damage, with deeper staining indicating more severe damage. The data are shown as the means of three independent biological replicates, with each replicate consisting of 5–6 individual plants. Error bars represent standard deviations of three independent biological replicates. (f) Relative electrolyte leakage (REL) and (g) Malondialdehyde (MDA) content of Micro-Tom WT, *SlNAC3*-overexpressing lines (OE#4/5/7) and *SlNAC3* CRISPR/Cas9 knock-out lines (*slnac3* #2/13) under different times of cold stress (4°C). Lowercase letters on the graphs indicate significant differences ($p < 0.05$, Duncan's test). (h) Phenotypes, (i) plant height and stem diameter of Micro-Tom WT and *SlNAC3*-overexpressing lines (OE#4/5) after 5 days of cold stress (4°C) recovery. [Color figure can be viewed at wileyonlinelibrary.com]
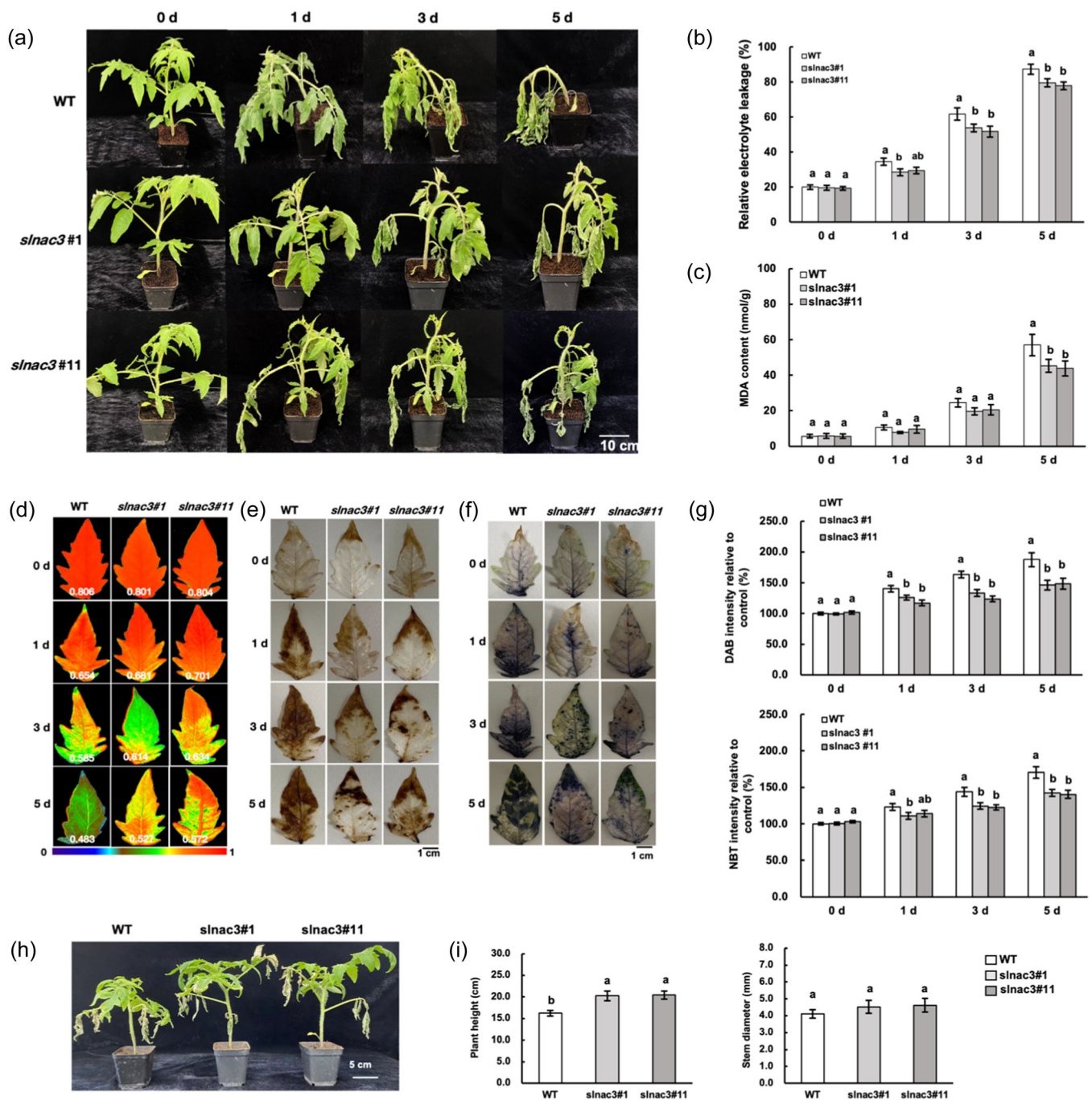
FIGURE 3 Phenotypic and physiological changes of Ailsa Craig WT and *SlNAC3* knock-out tomato under different times of cold stress. (a) Phenotypes of Ailsa Craig WT and CRISPR/Cas9 knock-out lines of *slnac3*#1/11 under different times of cold stress (4°C). Scale bar = 5 cm. (b) Relative electrolyte leakage (REL), (c) Malondialdehyde (MDA) content, and (d) Fv/Fm (maximum quantum yield of PSII) of Ailsa Craig WT and CRISPR/Cas9 knock-out lines of *slnac3*#1/11 under different times of cold stress (4°C). The colour change bar depicted at the bottom of the image represents the degree of damage in the leaves. Lowercase letters indicate more severe damage in the leaves. (e) DAB (3,3'-diaminobenzidine), (f) Nitro blue tetrazolium (NBT) staining and (g) Intensity of DAB and NBT relative to control (WT at 0 d) of tomato leaves. The blue colour on the leaves represents the degree of damage, with deeper staining indicating more severe damage. The data are shown as the means of three independent biological replicates, with each replicate consisting of 5-6 individual plants. Error bars represent standard deviations of three independent biological replicates. Lowercase letters on the graphs indicate significant differences ($p < 0.05$, Duncan's test). (h) Phenotypes, (i) Plant height and stem diameter of Ailsa Craig WT and CRISPR/Cas9 knock-out lines of *slnac3*#1/11 after 5 days of cold stress (4°C) recovery. [Color figure can be viewed at wileyonlinelibrary.com]
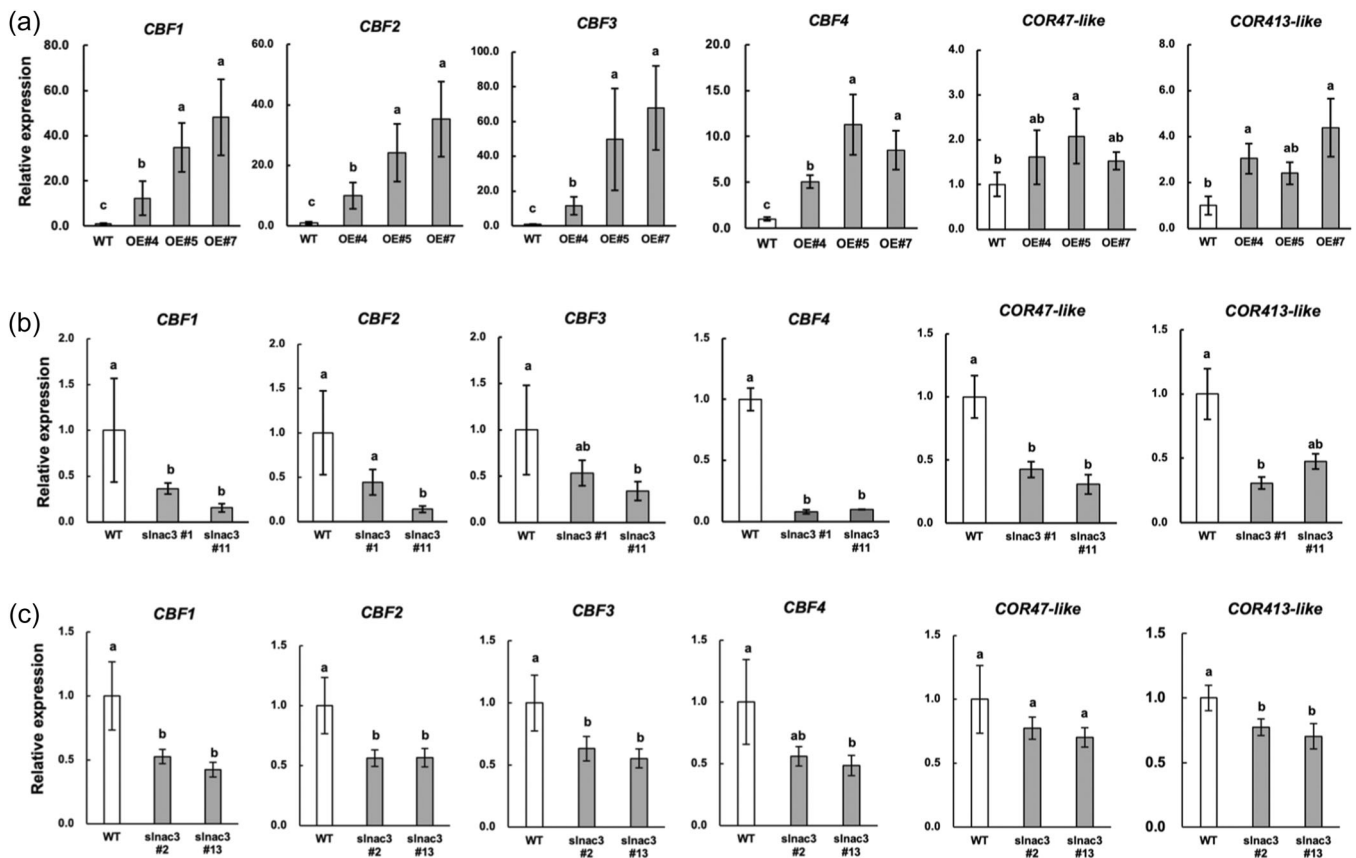
FIGURE 4 Relative expression levels of cold stress-responsive genes in WT and *SlNAC3* transgenic plants. Relative expression levels of cold stress-responsive genes in (a) Micro-Tom WT and *SlNAC3*-overexpressing lines (OE#4/5/7), (b) Ailsa Craig WT and CRISPR/Cas9 knock-out lines of *slnac3*#1/11, and (c) Micro-Tom WT and CRISPR/Cas9 knock-out lines of *slnac3* #2/13. *EF-1α* was used as the internal control. The data are shown as the means of three independent biological replicates. Error bars represent standard deviations of three independent biological replicates, with each replicate consisting of 5–6 individual plants. Lowercase letters on the graphs indicate significant differences ($p < 0.05$, Duncan's test).

SlNAC3 binding validation. To investigate whether SlNAC3 activates the transcription of these three genes, we performed LUC/REN assays using ACS2/4 as positive controls. The dual-luciferase reporter assay demonstrated that SlNAC3 could activate the expression of *SlACO1*, *SlACS2*, and *SlACS4* but not *SlACO3* and *SlACO4* (Figure 5e,f). To further validate the binding of SlNAC3 protein to the promoters of *SlACO1*, we conducted yeast one-hybrid assays for the three genes selected from the dual-luciferase reporter assay. The results showed that SlNAC3 could interact with the promoters of *SlACO1* (Figure 5g). Additionally, electrophoretic mobility shift assay (EMSA) was employed to detect the direct binding of the protein to DNA sequences. We synthesised 30-bp probes containing the "CACG" motifs from the promoters of *SlACO1*, with and without biotin labelling (Biotin-probe and cold-probe, respectively). Mutant probes with altered "CACG" sequences were also prepared (Mutant-probe). The EMSA results demonstrated that SlNAC3 could specifically bind to the "CACG" motifs in the promoter regions of *SlACO1* (Figure 5h). Additionally, yeast one-hybrid and EMSA assays also confirmed SlNAC3 could also bind to the "CACG" motifs in the promoter regions of *SlASC2/4* (Figure 5d, Figure S5a,b).

To further determine whether SlNAC3 could influence ethylene biosynthesis in tomato leaves, we measured the ethylene release rate in *SlNAC3* overexpression, knockout plants and wild-type plants. The results showed that the ethylene release rate was higher in the *SlNAC3* overexpression plants compared to the wild-type plants, but unaffected in the knockout lines (Figure 5i). These results are in line with the cold phenotype of *SlNAC3* transgenic lines (Figure 2), and suggest other players than SlNAC3 involved in ethylene production. Collectively, SlNAC3 exerts a positive regulatory role in the synthesis and release of ethylene in tomato plants by directly binding to the promoters of *SlACO1*, *SlACS2*, and *SlACS4*.

2.5 | SlNAC3 suppresses cold tolerance in tomato plants by enhancing ethylene biosynthesis

Ethylene level was measured in *SlNAC3*-overexpressing and wild-type tomato plants under both 25°C and 4°C. The results demonstrate that, under 25°C conditions, *SlNAC3*-overexpressing plants exhibited slightly higher ethylene release
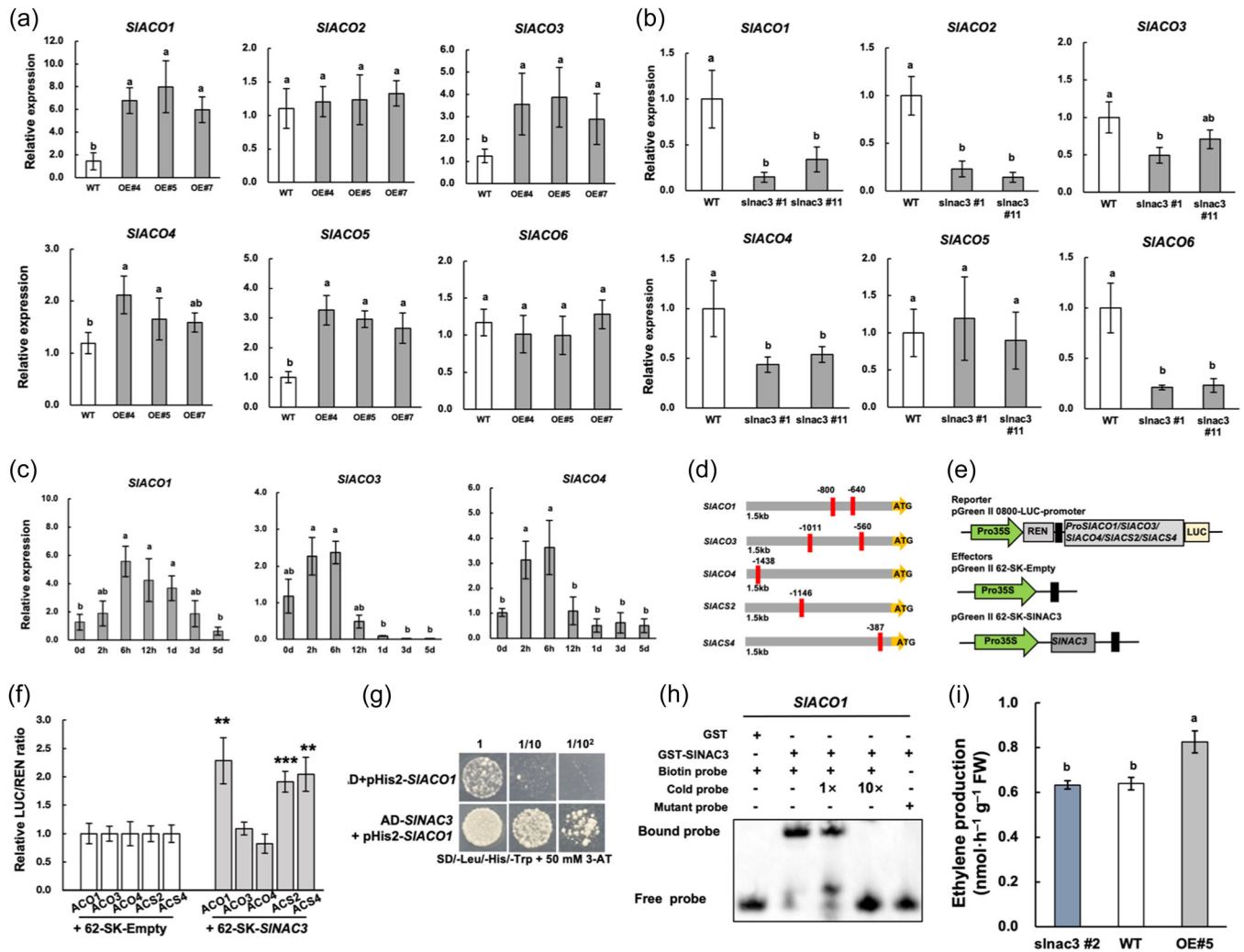
FIGURE 5 SlNAC3 directly binds to the promoters of SlACO1, SlACS2, and SlACS4 and regulates ethylene production. Relative expression levels of *SlACO1/2/3/4/5/6* in (a) Micro-Tom WT and *SlNAC3*-OE#4/5/7 plants and (b) Ailsa Craig WT and CRISPR/Cas9 knock-out lines *slnac*3#1/11. *EF-1α* was used as the internal control. The data are shown as the means of three independent biological replicates. Error bars represent standard deviations of three independent biological replicates, with each replicate consisting of 5–6 individual plants. Different small letters indicate significant differences ($p < 0.05$, Duncan's test). (c) Relative expression levels of *SlACO1/3/4* in Micro-Tom WT plants under cold stress (4°C) for 5 days. *EF-1α* was used as the internal control. The data are shown as the means of three independent biological replicates. Error bars represent standard deviations of three independent biological replicates, with each replicate consisting of 5–6 individual plants. Different small letters indicate significant differences ($p < 0.05$, Duncan's test). (d) Schematic diagram of the location of the NAC binding sequences (CACG or CGT(A/G)) of *SlACO1/3/4 and SlACS2/4* promoters within approximately 1.5 kb upstream sequences. The number represents the distance from the translation start sites. The location of CACG or CGT(A/G) is marked with a red bar on the schematic diagram of the promoters. (e) Schematic diagram of reporter and effector gene construction in Dual-luciferase assays. (f) The relative LUC/REN (firefly luciferase/Renilla luciferase) ratio for each group of Dual-luciferase assays. Asterisks indicate significant differences between each group (***$p < 0.001$, **$p < 0.01$, *$p < 0.05$, Student's t-test). (g) Yeast one-hybrid assays (Y1H). The promoters of *SlACO1* containing the putative NAC binding sequences were constructed in the pHis2 vector. The open reading frame (ORF) of SlNAC3 was constructed in the pGADT7 vector. Yeast cells were grown on SD/-Leu/-His/-Trp medium with 3-AT (3-amino-1,2,4-triazole) at a screened concentration. The data are shown as the means of three independent biological replicates. Error bars represent ± SD of three independent biological replicates, with each replicate consisting of 5–6 individual plants. (h) Electrophoretic mobility shift assay (EMSA). The GST-SlNAC3 and GST proteins were induced and purified through corresponding vectors and *E. coli* strains. GST proteins were used as a negative control. Biotin probes contained the NAC binding sequences and biotin label. Cold probes only contained the NAC binding sequences. Mutant probes in which the CACG or CGT(A/G) motif was changed to AAAA. The symbols + or – represent presence or absence, respectively. (i) Ethylene production of WT, *SlNAC3*-OE#5 and CRISPR/Cas9 knock-out lines *slnac*3#2 Micro-Tom plants at room temperature condition. The data are shown as the means of 3 independent biological replicates. Error bars represent ± SD of three independent biological replicates with each replicate being from 3 to 5 plants. Different small letters indicate significant differences ($p < 0.05$, Duncan's test). [Color figure can be viewed at wileyonlinelibrary.com]

rates at various time points compared to wild-type plants (Figure 6a). Similarly, under 4°C cold stress, ethylene release rates in *SINAC3*-overexpressing plants were consistently higher than in wild-type plants, with a significant increase observed after 6 h of exposure to 4°C (Figure 6b). Additionally, it was observed that both wild-type and overexpressing plants showed an overall increase in ethylene release under 4°C cold stress, followed by a subsequent decline (Figure 6b). Aligning with the transcription level of SINAC3 in response to cold (Figure 1a), these results suggest that SINAC3 plays an important role in cold responses by regulating ethylene production.

To further investigate whether the reduced cold tolerance in tomato plants is mediated by enhanced ethylene biosynthesis through SINAC3, we applied exogenously ACC, ETH, and the ethylene synthesis inhibitor 1-MCP. Continuous 3-day spraying and fumigation with ACC, ETH and 1-MCP were performed on wild-type tomato plants at the six-leaf stage, followed by 4°C cold treatment. The results indicated that both ACC and ETH treatments resulted in increased transcription levels of *SlACO1*, *SlACS2*, and *SlACS4* at different time points compared to the control group (Figure S6a–d). Additionally, on the fifth day of cold treatment, wild-type tomato plants treated with ACC and ETH exhibited more severe wilting and curling symptoms compared to the control group, while those subjected to 1-MCP fumigation displayed milder cold damage symptoms (Figure 6c). Moreover, the relative electrolyte leakage and MDA (malondialdehyde) content in tomato plants treated with ACC and ETH were significantly higher than in the control group on the fifth day of
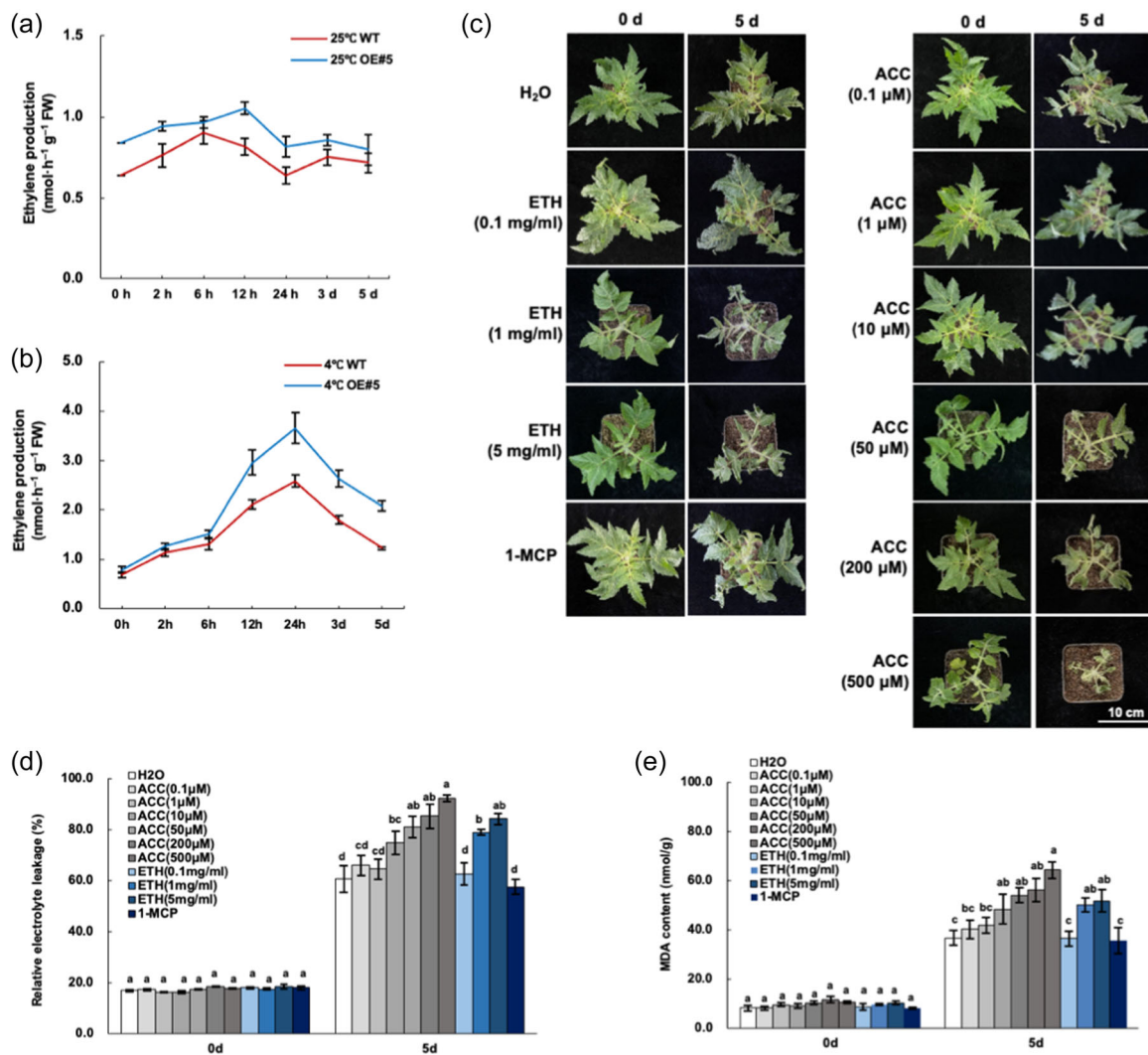

FIGURE 6 Effects of different exogenous ethylene treatments on the cold tolerance of tomato plants. (a) Ethylene production in leaves of WT and SINAC3-OE tomato plants at normal condition for 5 days. (b) Ethylene production in leaves of WT and SINAC3-OE tomato plants under cold stress (4°C) for 5 days. (c) Effects of different concentrations of ETH (ethylene), ACC (1-aminocyclopropane-1-carboxylic acid), and 1-MCP (1-methylcyclopropene) treatments on WT tomato plants under 5th-day cold and normal conditions. (d) Relative electrolyte leakage, and (e) Malondialdehyde (MDA) content of different concentrations of ETH, ACC, and 1-MCP treatments in WT tomato plants under the 5th-day cold and normal conditions. [Color figure can be viewed at wileyonlinelibrary.com]

4°C treatment, whereas the plants treated with 1-MCP exhibited not significantly difference of electrolyte leakage and MDA levels compared to the control group (Figure 6d,e). These results suggest that exogenous ACC and ETH treatments decrease cold tolerance in tomato plants, while 1-MCP fumigation in our experiment do not enhance their cold tolerance significantly.

We employed virus-induced gene silencing (VIGS) technology to silence the genes *SlACO1*, *SlACS2*, and *SlACS4* in tomato plants, selecting plants with silencing efficiency above 50% for the 4°C low-temperature treatment experiment. The results demonstrated that on the fifth day of the low-temperature treatment, the control group plants exhibited the most pronounced symptoms of leaf curling and wilting. In contrast, plants with silenced *SlACS2* and *SlACS4* genes displayed only mild leaf curling symptoms, while the symptoms of plants with silenced *SlACO1* genes were intermediate between the two group plants (Figure 7a). Additionally, the relative conductivity and malondialdehyde (MDA) levels of plants with silenced *SlACS2* and *SlACS4* genes were significantly lower than those of the control group and plants with silenced *SlACO1* gene, with no notable differences observed between the control group and plants with silenced *SlACO1* gene (Figure 7b,c). These results indicate that silencing the *SlACO1*, *SlACS2*, and *SlACS4* genes can enhance the cold tolerance of tomato plants.

3 | DISCUSSION

Under low temperature stress, plant cell membranes tend to transition from a liquid-crystalline state to a gel state. This change can lead to functional impairment of plant cells. Low temperature stress also has adverse effects on plant growth, development, and yield, especially for crops such as tomato that originated from tropical and subtropical regions. Currently, the NAC family is one of the transcription factor families found exclusively in plants, and its genes play important roles in plant growth, development, and response to environmental stresses. Studies have shown that NAC genes in tomato have both positive and negative regulatory roles in the plant's response to environmental stress (Olsen et al., 2005; Puranik et al., 2012).

Among the various NAC transcription factors, SlNAC3 stands out as a first-wave transcription factor that responds to low temperatures (Figure 1a), similar to the well-known CBFs. The induction of CBFs is generally associated with enhanced cold tolerance. However, *SlNAC3* overexpression led to decreased cold tolerance (Figures 2 and 3), despite higher expression levels of CBFs (Figure 4). Intriguingly, although a similar trend in CBF and COR expression exists, CBF1/2/3 were induced approximately 30 times in SlNAC3 overexpression lines, whereas the induction of COR genes is only about 2 times, and not all inductions are statistically significant
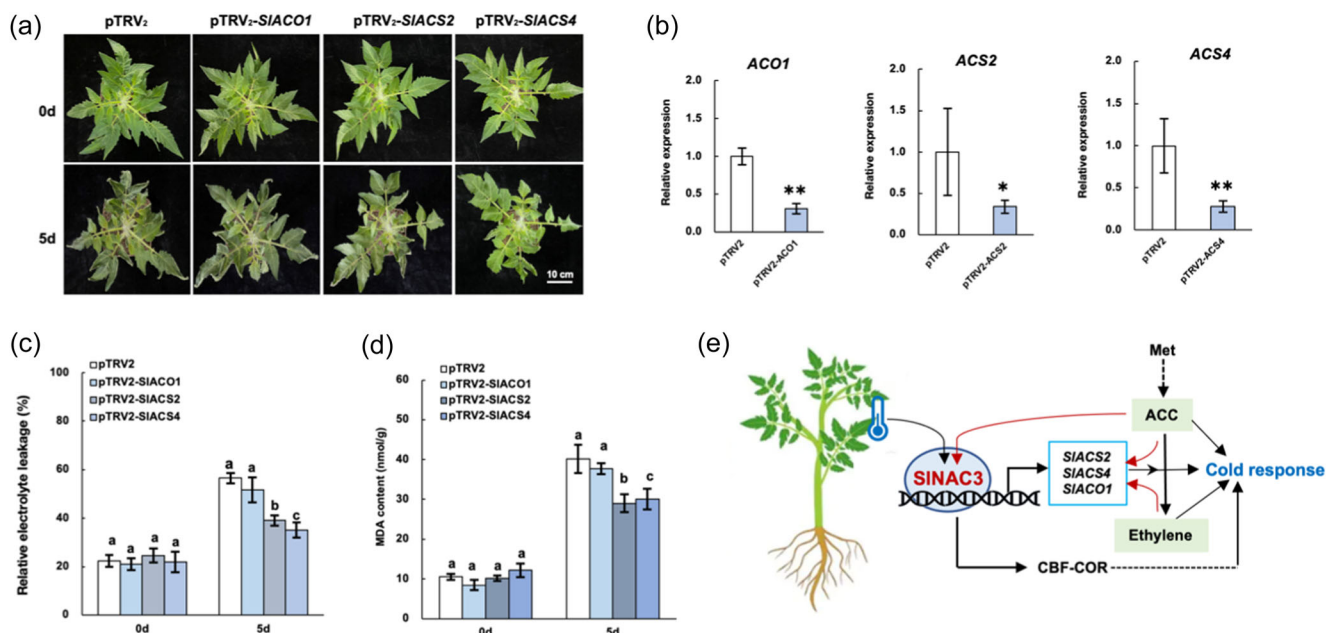

FIGURE 7 Effects of Virus-induced gene silencing of *SlACO1*, *SlACS2*, and *SlACS4* on the cold tolerance of tomato plants. (a) Phenotypes of pTRV, pTRV-ACO1, pTRV-ACS2, and pTRV-ACS4 tomato plants under cold stress (4°C) for 5 days. Scale bar = 5 cm. The Micro-Tom was used in the treatment. (b) Gene silencing efficiency of *SlACO1*, *SlACS2*, and *SlACS4* in tomato plants. Asterisks indicate significant differences between pTRV-ACO1 and pTRV plants, pTRV-ACS2, and pTRV plants, pTRV-ACS4, and pTRV plants (***$p < 0.001$, **$p < 0.01$, *$p < 0.05$, Student's *t*-test). EF-1α was used as the internal control. (c) Relative electrolyte leakage, and (d) Malondialdehyde (MDA) content of pTRV, pTRV-ACO1, pTRV-ACS2, and pTRV-ACS4 tomato plants under cold stress (4°C) for 5 days. The data are shown as the means of three independent biological replicates. Error bars represent ± SD of 3 independent biological replicates, with each replicate consisting of 5–6 plants. Different small letters indicate significant differences ($p < 0.05$, Duncan's test). (e) Schematic model of SlNAC3 participating in cold stress regulation of tomato plants. [Color figure can be viewed at wileyonlinelibrary.com]

(Figure 4). This paradox suggests that additional posttranscriptional mechanisms may be at play in the SlNAC3-mediated cold response. One such mechanism involves ribosome biogenesis factors, which confer cold tolerance by promoting the production of CBF proteins independently of transcriptional induction (Yu et al., 2020). This suggests that translational control of CBFs might play a role in the cold response mediated by SlNAC3. Notably, in eukaryotes, the target of rapamycin (TOR) kinase serves as a master regulator of protein synthesis and has been found to benefit plants under cold stress (Dong et al., 2019; Dong et al., 2023). Interestingly, inhibiting TOR resulted in the accumulation of ACS2 protein, indicating a negative regulatory role of TOR in ethylene signalling (Zhuo et al., 2020). In our study, we identified ACS2, as a crucial transcriptional target of SlNAC3 (Gao et al., 2018), regulates the cold tolerance of tomato plants (Figure 7). This finding is consistent with the observed impaired cold sensitivity upon ethylene application or TOR silencing (Dong et al., 2019). Investigating the role of the TOR signalling pathway in the regulatory networks governed by NAC transcription factors in response to cold stress holds promise for future research.

The pivotal roles of NAC transcription factors and ethylene signalling in fruit ripening are well-established. Among these factors, SlNAC3 has been identified as a key regulator of ethylene biosynthesis and cell wall modifications, crucial for tomato fruit softening and ripening (Gao et al., 2018). In our study, we made an intriguing discovery that SlNAC3 directly governs the transcription of ethylene biosynthesis genes, leading to compromised sensitivity to low temperatures (Figure 5). The previous study reported that the SlNAC3 (also known as NOR-like 1) mutation inhibited tomato fruit softening by reducing the transcription of pectinesterase SlPG2a and polygalacturonase SlPL involved in the cell wall metabolism (Gao et al., 2018). This may lead to the softening of stems and leaf veins in the SlNAC3 overexpressing plants (Figure 2a), thus contributing to their increased susceptibility to chilling stress symptoms in low-temperature conditions.

The involvement of ethylene in plant responses to low-temperature stress has been documented in various species, including tomato, tobacco, and Arabidopsis (Antonietta et al., 2023; Huang et al., 2023). In Arabidopsis, ethylene has been shown to negatively regulate freezing tolerance by repressing CBF expression (Shi et al., 2012). Another study reported that overexpression of tomato ShNAC1 increased sensitivity to low temperatures compared to the wild type. ShNAC1 upregulated three ACO genes and one ACS gene, suggesting its negative role in tomato's cold tolerance through modulation of ethylene biosynthesis (Liu et al., 2018). In contrast, the Arabidopsis acs mutant exhibited a freezing-sensitive phenotype (Catalá et al., 2014). SlNAM3 was found to increase the expression of SlACS1A, SlACS1B, SlACO1, and SlACO4, promoting ethylene synthesis and enhancing cold tolerance in tomato plants (Dong et al., 2022a). Catala and colleagues suggested that the discrepancy could be attributed to the high humidity in the petri dish system compared to the soil growth conditions (Catalá et al., 2014). However, both the tomato studies, including our own, were conducted with plants grown in soil. While ACC application has been demonstrated in several reports to mitigate chilling injury in tomatoes (Ding et al., 2022; Dong et al., 2022a; Liu et al., 2020), it is crucial to acknowledge that ethylene, as a stress response signalling molecule, exhibits a concentration-dependent effect on the regulation of plant cold tolerance (Pesis et al., 2002; Salvador et al., 2006). Furthermore, the cultivation and management conditions of plants, along with the concentration of exogenous substances, treatment time, and methods, may play varying roles in regulating plant cold sensitivity (Baker et al., 2022; Shi et al., 2012; Tsuchisaka et al., 2009).

Considering the dynamic nature of ethylene release during cold stress (Figure 6a), we speculate that the conflicting results can be resolved by analyzing temporal and spatial ethylene signalling in response to low temperatures. For example, SlNAC3 was the most induced after 2-h cold stress (Figure 1a), whereas NAM3 was discovered in a 6-h cold stress data set (Dong et al., 2022a). Additionally, we observed a feedback mechanism where elevated ethylene levels modulate the transcriptional regulation of ethylene biosynthesis genes (Figure S6). By integrating NACs into the central signalling pathway and gaining a better understanding of how NACs are regulated by various upstream factors, we can potentially resolve the contradictory findings regarding the roles of ethylene and NACs in plant cold tolerance. By elucidating these complex relationships, we can provide valuable insights and potentially reconcile the conflicting results, leading to a more coherent understanding of the roles of ethylene and NACs in plant cold tolerance.

Remarkably, a previous study proposed that ethylene signalling reciprocally regulates the expression of diverse NACs by removing a repressive histone mark H3K27me3 (Cao et al., 2021), established by the Polycomb repressive complex 2 (PRC2) (Bieluszewski et al., 2021). Notably, recent research has highlighted the TOR-PRC2 pathway as a critical player in plant development and stress responses (Dong et al., 2022b; Ye et al., 2022). Interestingly, TOR negatively modulates ethylene signalling (Zhuo et al., 2020), as demonstrated by a previous study of heightened ethylene levels and accelerated fruit ripening in tomato upon TOR silencing (Choi et al., 2022; Xiong et al., 2023). These findings lead us to speculate that the TOR-PRC2 pathway may exert an important regulatory role in the transcriptional network governed by NACs. By unravelling the complex interactions between NACs, TOR-PRC2 signalling, and ethylene signalling, it will enhance our understanding of the molecular mechanisms underlying the response to cold stress. Further exploration of these pathways will contribute to developing strategies to improve cold tolerance in crops and enhance their productivity in challenging environmental conditions.

4 | MATERIALS AND METHODS

4.1 | Plant materials and growth conditions

The tomato varieties used in this experiment were Micro Tom and Alisa Craig. The crispr knock-out SlNAC3 Alisa Craig tomato seeds

were provided by Prof. Daqi Fu of College of Food Science & Nutritional Engineering of China Agricultural University. Tomato seedlings were grown in a culture box under the following conditions: 26°C, 16 h light/18°C, 8 h dark, and relative humidity of 50%–80%. When the seedlings reached the six-leaf stage, they were subjected to cold treatment at 4°C. The cold treatment was carried out in the culture box under the conditions of 4°C, 16 h light/4°C, 8 h dark, and relative humidity of 50%–80%.

ACC (50 μM) and ethephon (0.1 mg/ml) solutions were prepared and continuously sprayed on tomato plants at the six-leaf stage for 3 days before the low-temperature treatment. For 1-MCP treatment, the inhibitor (1 μl/L) was dissolved in deionized water and fumigated in a closed container for 3 days before the low-temperature treatment.

4.2 | RNA extraction, reverse transcription, and RT-qPCR

Total RNA was extracted from tomato leaves using the Trizol method (Vazyme Biotech). The extracted RNA was quantified using Nano-Drop, and cDNA was synthesised using the Prime ScriptTM RT reagent Kit (Vazyme Biotech). RT-qPCR was performed using the QuantStudio 6 Flex instrument, and the $2^{-\Delta\Delta CT}$ method was used to analyze the expression of target genes. The SYBR fast Universal qPCR Kit (Vazyme Biotech) was used for RT-qPCR, with *EF-1α* chosen as the reference gene. Each sample was subjected to three biological replicates. The primer sequences used in this experiment are listed in Table S1.

4.3 | Construction and plant transformation

To create *SlNAC3* overexpression lines (*SlNAC3*-OE), the full-length cDNA *SlNAC3*(Solyc07G063420) was PCR amplified from Micro Tom and constructed into plant binary gateway vector pK7FWG2 by BP recombination reaction.

To create *SlNAC3* CRISPR/Cas9 knockout lines of Micro Tom, firstly, CRISPR/Cas9 targets was designed by using CRISPR/Cas9 online tools (http://www.crisprscan.org/?page=sequence, http://www.rgenome.net/cas-offinder/). Dual target expression sequence cassettes based on endogenous tRNA-processing strategy were synthesised as described in (Xie et al., 2015) and then ligated into pKSE401 vector. The fusion of U6 promoter with the dual target expression sequence cassettes was PCR amplified by using SlNAC3-2gRNA-F/R listed in Table S2. Then, the product was recombined with the single-digested product of pc131-35s-CAS9 vector with Hind III by using ClonExpress-II One Step Cloning Kit (Vazyme biotech Co.). The resulted products were transformed into *Ecoli*. DH5α and sequencing with primers 131Cas9-F and PKSE-ZJ-F.

Agrobacterium strain EHA105 carrying the pK7FWG2-SlNAC3-eGFP and pc131-35s-CAS9 recombinant vectors were used to infect tomato cotyledons. Subsequently, tissue culture was performed, and the tissue-cultured seedlings were transferred to soil for domestication. Leaf DNA was extracted from the domesticated plants for identification, and the expression level of *SlNAC3* in the plants was determined to obtain the T0 generation of *SlNAC3-OE*. The plants were further propagated to obtain the T2 generation of independent lines for subsequent experiments. The primer sequences used in this experiment are listed in Table S2.

4.4 | Measurement of physiological indices

When tomato seedlings reached the six-leaf stage, they were subjected to 4°C cold treatment. After treatment, the phenotypes of tomato plants were photographed, and the relative electrolyte leakage (REL) of the fourth true leaf was determined according to Liu et al. (2022) (Liu et al., 2022). The relative conductivity was calculated according to the formula: REL = (EC1−EC0)/(EC2−EC0) × 100%.

Malondialdehyde (MDA) content in tomato leaves was detected using the thiobarbituric acid (TBA) method as described by Liu et al. (2022) (Liu et al., 2022). Three true leaves from each of three seedlings were used as one biological replicate, and three biological replicates were performed for each treatment. MDA concentration was calculated using the formula: cMDA (μmol L^{-1}) = 6.45 × (OD532 − OD600) − 0.56 × OD450; MDA concentration in the extraction solution (μmol mL^{-1}) = (cMDA × volume of reaction solution)/(volume of extraction solution × 1000); MDA content (μmol/g FW) = (MDA concentration in the extraction solution × total volume of extraction solution)/sample fresh weight.

Maximum photochemical efficiency (Fv/Fm) of photosystem II was measured using a CF Imager-CF0077 chlorophyll fluorescence imaging system according to the method of Wang et al. (2019). The Fv/Fm value of the sixth true leaf of each plant was measured at each cold treatment time point, and six biological replicates were performed for each treatment.

DAB (3,3'-diaminobenzidine) and nitrotetrazolium blue chloride (NBT) staining were performed on the fifth true leaf of tomato seedlings following the steps described by Fryer et al. (2002). DAB and NBT reagents were purchased from Beijing Coolaber Company. For DAB staining, 50 mg of DAB was added to a 50 mL centrifuge tube containing 45 mL of distilled water, followed by the addition of 25 μL Tween-20 and 2.5 mL of 200 mM Na_2HPO_4 to the tube to prepare a 10 mM Na_2HPO_4-DAB solution. Three true leaves from each of three seedlings were used as one biological replicate, and three biological replicates were performed for each treatment. For NBT staining, 0.1 g of NBT was dissolved in 50 mL of 50 mM phosphate buffer to prepare a 0.2% NBT staining solution. The intensity of DAB and NBT staining was analyzed by using ImageJ. Three true leaves from each of three seedlings were used as one biological replicate, and three biological replicates were performed for each treatment.

4.5 | Ethylene release measurement

For measuring ethylene release, 0.8 g leaves of wild-type and *SlNAC3* overexpressing plants subjected to different time points of cold treatment were placed in a Schlenk flask and sealed in the dark for 1.5 h. The gas inside the flask was then transferred to a vacuum tube using a syringe, and the ethylene content was measured using a Shimadzu GC-2010 gas chromatograph. Chromatographic column: Capillary column, HP-5, 30 metres long, 0.32 millimetres inner diameter, with a membrane thickness of 0.5 μm; carrier gas: nitrogen; carrier gas flow rate: 4 mL/min; Injection method: no split flow; Detector: FID, detector gas is electronically controlled by APC; Detection amount: 3pgC/s (dodecane); Pressure setting range: 0–970KPa; Flow setting range; 0–1200 mL/min; Oven temperature: 35°C; Injector temperature: 220°C; Ion source temperature: 250°C; Interface temperature: 250°C; Analysed mass domain: 50–200 m/z; Detector sensibility: 1.05 V. The calculation formula of chromatograph setting is as follows:

$$\text{Ethylene release rate (nmol h}^{-1}\text{ g}^{-1}\text{ FW)}$$
$$= A \times A \times V \div T \div M,$$

A is the peak area of ethylene; A is the slope of the ethylene standard curve, with a value of 0.0236 nmol mL^{-1}, V is the volume of the container (mL); T is the sealed incubation time (h); M is the fresh weight of the sample (g).

4.6 | Yeast one-hybrid assay

The 1.5 kb promoter sequence containing NAC protein binding motifs of the target gene was cloned into the pHis2 vector as the bait vector, and the CDS sequence of *SlNAC3* was cloned into pGADT7 as the prey vector. Different recombinant vectors were transformed into Y187 yeast strain, and the yeast strains were selected on SD/-H/-L/-T medium containing 3-AT at appropriate inhibitory concentrations. The pGADT7 empty vector was used as a negative control. The bait and prey vectors from the control group and experimental group were co-transformed into Y187 yeast strain, and the yeast strains were cultured on SD/-H/-L/-T medium containing 3-AT at appropriate inhibitory concentrations. The experiment was repeated three times.

4.7 | Dual-luciferase assay

The CDS sequence of *SlNAC3* was cloned into the pGreenII 62-SK vector, and the 1.5 kb upstream region sequence of the target gene was cloned into the pGreenII 0800-LUC vector. The recombinant vectors were validated by sequencing and then transformed into *Agrobacterium* (GV3101). Tobacco leaves were co-injected with *Agrobacterium* containing pGreenII 62-SK and pGreenII 0800-LUC with or without the 1.5 kb upstream region sequence of the target gene.

After 2 days of incubation, leaf samples were taken from the injection site and processed following the instructions of the Dual-Luciferase Assay Kit (Vazyme). The firefly luciferase (LUC) and Renilla luciferase (REN) values were measured using a multifunctional microplate reader. The experiment was repeated three times.

4.8 | Electrophoretic mobility shift assay (EMSA)

The CDS sequence of *SlNAC3* was cloned into the pGEX-4T-2 vector, and the recombinant vector was transformed into *Escherichia coli* strain BL21 (DE3). The SlNAC3-GST fusion protein expression was induced and purified using an appropriate concentration of isopropyl β-D-1-thiogalactopyranoside (IPTG) and induction temperature. Probes with 30 bp sequences containing "CACG" or "CGT(A/G)" motifs in the target gene promoter were synthesised with biotin labelling. Probes without biotin labelling were used as cold probes, and probes with mutations changing "CACG" sequence to "AAAA" were used as mutant probes. EMSA reaction was performed following the instructions of the EMSA kit (Thermo Fisher). The probe sequences used in this experiment are listed in Table S3.

4.9 | Virus-induced gene silencing (VIGS)

Specific sequences from the CDS of the target gene were cloned into the pTRV2 vector and transformed into Agrobacterium GV3101. Tomato seedlings at the one-leaf stage were injected with a mixture of Agrobacterium containing pTRV1 and pTRV2 recombinant plasmids. The inoculated tomato seedlings were placed in a growth chamber for cultivation. pTRV2 was used as a negative control, and pTRV2-PDS was used as a positive control. When the plants grew to the four-leaf stage, the presence of TRV1 and TRV2 vectors in the plants was detected, and the silencing efficiency was verified using RT-qPCR. Plants with relatively high silencing efficiency were selected for subsequent low-temperature treatment experiments.

4.10 | Data processing and analysis

All statistical data in this study, including mean, standard deviation, and significance, were analyzed using SPSS (version 25) and Excel (Office 2010). Duncan's multiple range test ($p < 0.05$) or independent samples t-test was used to determine the significance between samples.

4.11 | Accession numbers

The accession numbers of all genes used in this paper were obtained from the Sol Genomics Network (Solanum_lycopersicum SL4.0 https://solgenomics.net/). They were listed in Table S1.

DATA AVAILABILITY STATEMENT

All data generated during this study are included within the article or its supplementary files.

ORCID

Xuemin Ma http://orcid.org/0000-0001-5690-7929

Wenna Zhang http://orcid.org/0000-0003-4094-9766

REFERENCES

An, J.P., Yao, J.F., Xu, R.R., You, C.X., Wang, X.F. & Hao, Y.J. (2018) An apple NAC transcription factor enhances salt stress tolerance by modulating the ethylene response. *Physiologia Plantarum*, 164, 279–289.

Antonietta, M., de Felipe, M., Rothwell, S.A., Williams, T.B., Skilleter, P., Albacete, A. et al. (2023) Prolonged low temperature exposure desensitises ABA-induced stomatal closure in soybean, involving an ethylene-dependent process. *Plant, Cell & Environment*, 46(7), 2128–2141.

Baker, C.R., Stewart, J.J., Amstutz, C.L., Ching, L.G., Johnson, J.D., Niyogi, K.K. et al. (2022) Genotype-dependent contribution of CBF transcription factors to long-term acclimation to high light and cool temperature. *Plant, Cell & Environment*, 45, 392–411.

Bieluszewski, T., Xiao, J., Yang, Y. & Wagner, D. (2021) PRC2 activity, recruitment, and silencing: a comparative perspective. *Trends in Plant Science*, 26, 1186–1198.

Cao, X., Wei, C., Duan, W., Gao, Y., Kuang, J., Liu, M. et al. (2021) Transcriptional and epigenetic analysis reveals that NAC transcription factors regulate fruit flavor ester biosynthesis. *The Plant Journal*, 106, 785–800.

Catalá, R., López-Cobollo, R., Mar Castellano, M., Angosto, T., Alonso, J.M., Ecker, J.R. et al. (2014) The arabidopsis 14-3-3 protein rare cold inducible 1A links low-temperature response and ethylene biosynthesis to regulate freezing tolerance and cold acclimation. *The Plant Cell*, 26, 3326–3342.

Choi, I., Ahn, C.S., Lee, D.H., Baek, S.A., Jung, J.W., Kim, J.K. et al. (2022) Silencing of the target of rapamycin complex genes stimulates tomato fruit ripening. *Molecules and Cells*, 45, 660–672.

Christiansen, M.W. & Gregersen, P.L. (2014) Members of the barley NAC transcription factor gene family show differential co-regulation with senescence-associated genes during senescence of flag leaves. *Journal of Experimental Botany*, 65, 4009–4022.

Ding, F., Wang, C., Xu, N. & Wang, M. (2022) The ethylene response factor SlERF.B8 triggers jasmonate biosynthesis to promote cold tolerance in tomato. *Environmental and Experimental Botany*, 203, 105073.

Ding, Y., Shi, Y. & Yang, S. (2019) Advances and challenges in uncovering cold tolerance regulatory mechanisms in plants. *New Phytologist*, 222, 1690–1704.

Dong, Y., Teleman, A.A., Jedmowski, C., Wirtz, M. & Hell, R. (2019) The Arabidopsis THADA homologue modulates TOR activity and cold acclimation. *Plant Biology*, 21, 77–83. Available from: https://doi.org/10.1111/plb.12893

Dong, Y., Tang, M., Huang, Z., Song, J., Xu, J., Ahammed, G.J. et al. (2022a) The miR164a-NAM3 module confers cold tolerance by inducing ethylene production in tomato. *The Plant Journal*, 111, 440–456.

Dong, Y., Uslu, V.V., Berr, A., Singh, G., Papdi, C., Steffens, V.A. et al. (2022b) TOR represses stress responses through global regulation of H3K27 trimethylation in plants. *Journal of Experimental Botany*, 74(5), 1420–1431.

Dong, Y., Srour, O., Lukhovitskaya, N., Makarian, J., Baumberger, N., Galzitskaya, O. et al. (2023) Functional analogs of mammalian 4E-BPs reveal a role for TOR in global plant translation. *Cell Reports*, 42, 112892.

Fryer, M.J., Oxborough, K., Mullineaux, P.M. & Baker, N.R. (2002) Imaging of photo-oxidative stress responses in leaves. *Journal of Experimental Botany*, 53, 1249–1254.

Gao, Y., Wei, W., Zhao, X., Tan, X., Fan, Z., Zhang, Y. et al. (2018) A NAC transcription factor, NOR-like1, is a new positive regulator of tomato fruit ripening. *Horticulture Research*, 5, 75.

Han, Q., Zhang, J., Li, H., Luo, Z., Ziaf, K., Ouyang, B. et al. (2012) Identification and expression pattern of one stress-responsive NAC gene from *Solanum lycopersicum*. *Molecular Biology Reports*, 39, 1713–1720.

Hao, Y.J., Wei, W., Song, Q.X., Chen, H.W., Zhang, Y.Q., Wang, F. et al. (2011) Soybean NAC transcription factors promote abiotic stress tolerance and lateral root formation in transgenic plants. *The Plant Journal*, 68, 302–313.

He, X.J., Mu, R.L., Cao, W.H., Zhang, Z.G., Zhang, J.S. & Chen, S.Y. (2005) AtNAC2, a transcription factor downstream of ethylene and auxin signaling pathways, is involved in salt stress response and lateral root development. *The Plant Journal*, 44, 903–916.

Hong, Y., Zhang, H., Huang, L., Li, D. & Song, F. (2016) Overexpression of a stress-responsive NAC transcription factor gene ONAC022 improves drought and salt tolerance in rice. *Frontiers in Plant Science*, 7, 4.

Huang, J., Zhao, X., Bürger, M., Chory, J. & Wang, X. (2023) The role of ethylene in plant temperature stress response. *Trends in Plant Science*, 28, 808–824.

Larran, A.S., Pajoro, A. & Qüesta, J.I. (2023) Is winter coming? Impact of the changing climate on plant responses to cold temperature. *Plant, Cell & Environment*, 46, 3175–3193.

Li, H., Ye, K., Shi, Y., Cheng, J., Zhang, X. & Yang, S. (2017) BZR1 positively regulates freezing tolerance via CBF-dependent and CBF-independent pathways in arabidopsis. *Molecular Plant*, 10, 545–559.

Liu, H., Zhou, Y., Li, H., Wang, T., Zhang, J., Ouyang, B. et al. (2018) Molecular and functional characterization of ShNAC1, an NAC transcription factor from *Solanum habrochaites*. *Plant Science*, 271, 9–19.

Liu, Q., Kasuga, M., Sakuma, Y., Abe, H., Miura, S., Yamaguchi-Shinozaki, K. et al. (1998) Two transcription factors, DREB1 and DREB2, with an EREBP/AP2 DNA binding domain separate two cellular signal transduction pathways in drought- and low-temperature-responsive gene expression, respectively, in arabidopsis. *The Plant Cell*, 10, 1391–1406.

Liu, W., Wang, Q., Zhang, R., Liu, M., Wang, C., Liu, Z. et al. (2022) Rootstock-scion exchanging mRNAs participate in the pathways of amino acids and fatty acid metabolism in cucumber under early chilling stress. *Horticultural Research*, 9, uhac031. https://doi.org/10.1093/hr/uhac031

Liu, Y., Zhang, L., Meng, S., Liu, Y., Zhao, X., Pang, C. et al. (2020) Expression of galactinol synthase from ammopiptanthus nanus in tomato improves tolerance to cold stress. *Journal of Experimental Botany*, 71, 435–449.

Ma, N.N., Zuo, Y.Q., Liang, X.Q., Yin, B., Wang, G.D. & Meng, Q.W. (2013) The multiple stress-responsive transcription factor SlNAC1 improves the chilling tolerance of tomato. *Physiologia Plantarum*, 149, 474–486.

Marti, E. (2006) Genetic and physiological characterization of tomato cv. Micro-Tom. *Journal of Experimental Botany*, 57, 2037–2047.

Oh, S.K., Lee, S., Yu, S.H. & Choi, D. (2005) Expression of a novel NAC domain-containing transcription factor (CaNAC1) is preferentially associated with incompatible interactions between chili pepper and pathogens. *Planta*, 222, 876–887.

Olsen, A.N., Ernst, H.A., Leggio, L.L. & Skriver, K. (2005) NAC transcription factors: structurally distinct, functionally diverse. *Trends in Plant Science*, 10, 79–87.

Pattyn, J., Vaughan-Hirsch, J. & Van de Poel, B. (2021) The regulation of ethylene biosynthesis: a complex multilevel control circuitry. *New Phytologist*, 229, 770–782.

Pesis, E., Ackerman, M., Ben-Arie, R., Feygenberg, O., Feng, X., Apelbaum, A. et al. (2002) Ethylene involvement in chilling injury symptoms of avocado during cold storage. *Postharvest Biology and Technology*, 24, 171–181.

Puranik, S., Sahu, P.P., Srivastava, P.S. & Prasad, M. (2012) NAC proteins: regulation and role in stress tolerance. *Trends in Plant Science*, 17, 369–381.

Ricachenevsky, F.K., Menguer, P.K. & Sperotto, R.A. (2013) kNACking on heaven's door: how important are NAC transcription factors for leaf senescence and Fe/Zn remobilization to seeds? *Frontiers in Plant Science*, 4, 226.

Salvador, A., Carvalho, C.P., Monterde, A. & Martìnez-Jávega, J.M. (2006) Note. 1-MCP effect on chilling injury development in 'nova' and 'ortanique' mandarins. *Food Science and Technology International*, 12, 165–170.

Shan, W., Kuang, J.F., Lu, W.J. & Chen, J.Y. (2014) Banana fruit NAC transcription factor MaNAC1 is a direct target of MaICE1 and involved in cold stress through interacting with MaCBF1. *Plant, Cell & Environment*, 37, 2116–2127.

Shi, Y., Tian, S., Hou, L., Huang, X., Zhang, X., Guo, H. et al. (2012) Ethylene signaling negatively regulates freezing tolerance by repressing expression of CBF and type-A ARR genes in arabidopsis. *The Plant Cell*, 24, 2578–2595.

Stockinger, E.J., Gilmour, S.J. & Thomashow, M.F. (1997) *Arabidopsis thaliana* CBF1 encodes an AP2 domain-containing transcriptional activator that binds to the C-repeat/DRE, a cis-acting DNA regulatory element that stimulates transcription in response to low temperature and water deficit. *Proceedings of the National Academy of Sciences*, 94, 1035–1040.

Tsuchisaka, A., Yu, G., Jin, H., Alonso, J.M., Ecker, J.R., Zhang, X. et al. (2009) A combinatorial interplay among the 1-aminocyclopropane-1-carboxylate isoforms regulates ethylene biosynthesis in *Arabidopsis thaliana*. *Genetics*, 183, 979–1003.

Wang, F., Zhang, L., Chen, X., Wu, X., Xiang, X. & Zhou, J. (2019) SlHY5 integrates temperature, light, and hormone signaling to balance plant growth and cold tolerance. *Plant Physiology*, 179, 749–760.

Wang, Z., Hong, Y., Yao, J., Huang, H., Qian, B., Liu, X. et al. (2022) Modulation of plant development and chilling stress responses by alternative splicing events under control of the spliceosome protein SmEb in *Arabidopsis*. *Plant, Cell & Environment*, 45, 2762–2779.

Xie, K., Minkenberg, B. & Yang, Y. (2015). Boosting CRISPR/Cas9 multiplex editing capability with the endogenous tRNA-processing system. *Proceedings of the National Academy of Sciences of the United States of America*, 112, 3570–3575.

Xia, N., Zhang, G., Liu, X.Y., Deng, L., Cai, G.L., Zhang, Y. et al. (2010) Characterization of a novel wheat NAC transcription factor gene involved in defense response against stripe rust pathogen infection and abiotic stresses. *Molecular Biology Reports*, 37, 3703–3712.

Xiong, F., Tian, J., Wei, Z., Deng, K., Li, Y. & Zhang, Y. (2023) Suppression of the target of rapamycin kinase accelerates tomato fruit ripening through reprogramming the transcription profile and promoting ethylene biosynthesis. *Journal of Experimental Botany*, 74, 2603–2619.

Ye, R., Wang, M., Du, H., Chhajed, S., Koh, J., Liu, K. et al. (2022) Glucose-driven TOR–FIE–PRC2 signalling controls plant development. *Nature*, 609, 986–993.

Yu, H., Kong, X., Huang, H., Wu, W., Park, J., Yun, D.J. et al. (2020) STCH4/REIL2 confers cold stress tolerance in arabidopsis by promoting rRNA processing and CBF protein translation. *Cell Reports*, 30, 229–242. e5.

Zhang, X., Long, Y., Huang, J. & Xia, J. (2020) OsNAC45 is involved in ABA response and salt tolerance in rice. *Rice (New York, N.Y.)*, 13, 79.

Zhao, C., Zhang, Z., Xie, S., Si, T., Li, Y. & Zhu, J.K. (2016) Mutational evidence for the critical role of CBF transcription factors in cold acclimation in arabidopsis. *Plant Physiology*, 171, 2744–2759.

Zhong, R., Lee, C. & Ye, Z.H. (2010) Evolutionary conservation of the transcriptional network regulating secondary cell wall biosynthesis. *Trends in Plant Science*, 15, 625–632.

Zhuo, F., Xiong, F., Deng, K., Li, Z. & Ren, M. (2020) Target of rapamycin (TOR) negatively regulates ethylene signals in arabidopsis. *International Journal of Molecular Sciences*, 21, 2680.

SUPPORTING INFORMATION

Additional supporting information can be found online in the Supporting Information section at the end of this article.